AGU PUBLICATIONS

Geophysical Research Letters

RESEARCH LETTER
10.1002/2016GL069569

Key Points:
- A new classification of stratospheric extreme events according to the significance of their impact on the troposphere is presented
- Only few (20%) of all stratospheric extreme events have a significant impact on the troposphere
- The impact on the troposphere does not depend on the strength but on the persistence of the stratospheric perturbation

Correspondence to:
H. Garny,
hella.garny@dlr.de

Citation:
Runde, T., M. Dameris, H. Garny, and D. E. Kinnison (2016), Classification of stratospheric extreme events according to their downward propagation to the troposphere, *Geophys. Res. Lett.*, *43*, 6665–6672, doi:10.1002/2016GL069569.

Received 12 MAY 2016
Accepted 11 JUN 2016
Accepted article online 15 JUN 2016
Published online 30 JUN 2016

Classification of stratospheric extreme events according to their downward propagation to the troposphere

T. Runde[1], M. Dameris[1], H. Garny[1], and D. E. Kinnison[2]

[1]Deutsches Zentrum für Luft- und Raumfahrt, Institut für Physik der Atmosphäre, Oberpfaffenhofen, Germany, [2]National Center for Atmospheric Research, Boulder, USA

Abstract This study presents a classification of stratospheric extreme events during northern winter into events with or without a consistent downward propagation of anomalies to the troposphere. Anomalous strong and weak stratospheric polar vortex events are detected from daily time series of the polar cap averaged (60°–90°N) geopotential height anomaly. The method is applied to chemistry-climate model data (E39CA and WACCM3.5) and reanalyses data (ERA40). The analyses show that in about 80% of all events no significant tropospheric response can be detected. The stratospheric perturbation of both weak and strong events with a significant tropospheric response persists significantly longer throughout the stratosphere compared to the events without a tropospheric response. The strength of the stratospheric perturbation determines the strength of the tropospheric response only to a small degree. Results are consistent across all three data sets.

1. Introduction

Dynamical extreme situations of the stratospheric polar vortex during northern winter are known to have an impact on tropospheric dynamics [*Baldwin and Dunkerton*, 1999, 2001; *Kidston et al.*, 2015]. These stratospheric events occur in the form of either a weakening of the polar vortex, i.e., sudden stratospheric warmings, or a strengthening of the polar vortex, i.e., polar vortex intensifications.

During northern winter the polar vortex has been shown to have a strong impact on the North Atlantic Oscillation (NAO) and consequently on tropospheric weather [*Rind et al.*, 2005; *Scaife et al.*, 2005; *Thompson et al.*, 2005; *Kolstad et al.*, 2010; *Hardiman et al.*, 2012]. This downward influence potentially leads to improved weather prediction following significant perturbations of the polar vortex [*Baldwin et al.*, 2003; *Hardiman et al.*, 2011; *Sigmond et al.*, 2013]. However, it is known that there is a high case-to-case variability in the strength of the downward propagation of the signal [*Nakagawa and Yamazaki*, 2006; *Gerber et al.*, 2009]; i.e., some stratospheric extreme events induce anomalies in the NAO and some do not.

The different behavior of the downward propagation of the stratospheric signal to the troposphere was examined for weak polar vortex events in model data [*Song and Robinson*, 2006] and ERA40 reanalysis data [*Nakagawa and Yamazaki*, 2006]. Both studies state that tropospheric wave forcing is essential to produce the tropospheric anomalies.

Several studies investigated the relation of the tropospheric response to properties of stratospheric extreme events. For example, *Mitchell et al.* [2013] showed that the behavior of the tropospheric response depends on the type of major stratospheric warmings, i.e., a vortex displacement or a vortex split. *Hitchcock et al.* [2013] classified stratospheric sudden warming events according to the depth of the initial perturbation and showed that events that initially penetrate to the lower stratosphere typically persist longer and have a stronger tropospheric response. A similar conclusion was found by *Gerber et al.* [2009], who furthermore showed that the tropospheric response to sudden warmings can easily be masked by the strong internal variability of the troposphere. Other studies emphasized the role of the tropospheric state for the downward propagation, such as *Garfinkel et al.* [2013], who found that the position of the tropospheric jet influences its response to stratospheric perturbations. In general, the mechanisms for the downward propagation of stratospheric perturbations remain still unclear. The most common explanation is the interaction between changes in

conditions for planetary wave propagation due to changes in the zonal mean flow [*Holton*, 2004; *Limpasuvan et al.*, 2004, 2005]. Recent studies emphasized the role of tropospheric eddy feedback for the downward propagation of stratospheric anomalies, both on synoptic [*Domeisen et al.*, 2013] and on planetary scales [*Hitchcock and Simpson*, 2014].

The present study introduces an approach to cluster stratospheric extreme events according to their tropospheric response rather than according to properties of the stratospheric extreme event itself. In particular, both weak and strong polar vortex events in the stratosphere are differentiated into events that do or do not show a consistent downward propagation of significant anomalies to the troposphere (700 hPa). The aim is to investigate whether there are robust differences between situations in which stratospheric extreme events have a significant impact on the tropospheric circulation or situations in which no such response can be detected.

2. Data and Methodology

2.1. Models and Reanalysis Data

This study is based on long-term simulations from the Chemistry-Climate models (CCMs) E39CA (ECHAM4.L39-(DLR)/CHEM/ATTILA) and WACCM3.5 (Whole-Atmosphere Chemistry-Climate Model, version 3.5) and on ERA40 reanalysis data. The used simulations were part of the second CCM validation activity (CCMVal2) of the Stratospheric Processes and Their Role in Climate project. Long data sets are required in this study since a sufficient number of extreme stratospheric events is needed to obtain statistical relevant result.

The CCM E39CA is based on the spectral general circulation model ECHAM4.L39(DLR) and the chemistry module CHEM [*Stenke et al.*, 2009]. The spectral horizontal resolution is T30 (3.75 × 3.75 latitude-longitude grid) and 39 layers extend from the surface to the uppermost layer centered at 10 hPa (about 30 km). The model reasonably represents both the mean climatological state and the interannual dynamical variability of the northern hemisphere with regard to reanalysis data sets, although E39CA does not resolve the entire stratosphere [*Dameris et al.*, 2005; *Stenke et al.*, 2009].

The transient simulations with E39CA used here follow the REF-B1, the SCN-B2c, and the SCN-B2d scenarios as defined in *Eyring et al.* [2008]. REF-B1 is designed to reproduce the past from 1960 to 2004 including anthropogenic and natural forcing. SCN-B2d spans from 1960 to 2049, and the future period (after 2000) follows the A1B scenario [*Nakicenovic and Swart*, 2000]. SCN-B2c (often called "No Climate Change" simulation) spans from 1960 to 2049. In contrast to SCN-B2d, Greenhouse gas concentrations in SCN-B2c are fixed at the level in year 1960 for the whole simulation period. Although the three simulations from E39CA are not performed with an identical setup of boundary conditions, they all are included in the composite analysis performed in this study because it turned out that the dynamic statistics of all three simulations are very similar and therefore can be combined to a consistent data set [*Runde*, 2012].

The CCM WACCM3.5 is based on the Community Atmosphere Model, version 3.5 (CAM3.5) with the vertical model domain spanning from surface up to 145 km on 66 vertical levels. The horizontal resolution for WACCM3.5 simulations in this study is a 1.9° × 2.5° latitude-longitude grid. The northern hemispheric interannual variability and the frequency of sudden stratospheric warmings are close to observations [*Richter et al.*, 2010]. For more details on the base model WACCM see *Garcia et al.* [2007].

For the present study with WACCM3.5, a three-member ensemble of transient simulation from 1953 to 2006 is used to reproduce the past also including anthropogenic and natural forcings as in REF-B1 of E39CA (hereafter refb1.1, refb1.2, and refb1.3). Details of the setup of those simulations can be found in *Garcia et al.* [2007].

The ERA40 reanalysis data set is a global data set that spans from September 1957 to August 2002. We used 6-hourly data with a horizontal resolution of 2.5° × 2.5° and the data expand from surface up to 1 hPa (about 50 km) on 23 pressure levels. They are produced with an assimilation procedure with the European Centre for Medium-Range Weather Forecasts (ECMWF) Integrated Forecasting System. ERA40 includes all appropriate and available observations of meteorological offices, radiosondes, and ship measurements. Since the 1970s, satellite measurements are also considered. A detailed description of the ERA40 reanalysis data is found in *Uppala et al.* [2005].

2.2. Methodology

The variability of the impact of stratospheric extreme events on tropospheric dynamics during northern winter situations is investigated in terms of a composite study. Commonly, the analysis method described by

Baldwin and Dunkerton [2001] is used to classify the dynamical state of the stratosphere into situations of an intensification of the polar vortex (strong vortex event) with higher zonal stratospheric west winds than on average and situations of a weakening of the polar vortex (weak vortex event) with a wind reversal from west to east zonal winds (sudden major warming) or at least a significantly reduced zonal west wind (i.e., strong minor warmings). The method from *Baldwin and Dunkerton* [2001] used the time series of the first empirical orthogonal function (EOF) of the 90 day low-pass-filtered geopotential height (hereafter GpH) anomaly between 20°N and 90°N. This coincides with the Northern Annular Mode (NAM) index. *Baldwin and Thompson* [2009] showed that using the zonally averaged GpH or zonal wind anomaly instead of the NAM index gives almost identical results.

We calculate both the daily anomaly of polar cap GpH (60°N–90°N) and the NAM (or Arctic Oscillation) index as described by *Baldwin and Dunkerton* [1999] (via EOF analysis of a latitude-longitude field) for the E39CA model, the WACCM3.5 model, and ERA40 data at 30 hPa. Due to the fact that the model E39CA has a top height at 10 hPa and to exclude wrong interpretation, the NAM index and the polar cap GpH anomaly are determined at 30 hPa instead of at 10 hPa. For WACCM3.5 and ERA40, the normalized time series at 30 hPa and 10 hPa are very similar. The interannual and intra-annual variability and amplitudes of the GpH anomalies and of the NAM Index are similar in all three data sets (not shown). The GpH and NAM time series are strongly anticorrelated (correlation coefficient is very close to −1.00 for all data sets), in agreement with *Baldwin and Thompson* [2009]. For the analysis in the following, the polar cap GpH anomaly is used.

For the new analysis method that allows for differentiation of the stratospheric and tropospheric dynamical state, two reference levels are chosen. The stratospheric dynamical state is represented by the detrended 90 day low-pass-filtered GpH anomaly over the polar cap at 30 hPa for all three data sets. If this stratospheric time series exceeds the positive (negative) value of 1.5 standard deviation for at least 10 consecutive days, a weak (strong) vortex event is detected. The threshold values of ± 1.5 standard deviation differ to the thresholds used in *Baldwin and Dunkerton* [2001], who used $+1.5\sigma$ and -3σ to detect strong (weak) vortex events. One reason for us to use symmetric sigma values is that the application of asymmetric threshold values leads to lower numbers of weak vortex events compared to strong vortex events, so that statistics for weak vortex events are less robust. However, the results shown in the following are independent of this choice of the threshold, as will be discussed in more detail at the end of the next section. Another choice we make is on the minimal persistence of the stratospheric threshold exceedance, here chosen as 10 days.

In the following, the date of the maximum (minimum) of the GpH anomaly in the stratosphere during the exceedance of the threshold value is defined as the stratospheric central day of the weak (strong) vortex event. For each event, the time series of the detrended 90 day low-pass-filtered GpH anomaly over the polar cap at each level below the stratospheric reference level (30 hPa) is analyzed for threshold exceedance above 1.5 standard deviation following the stratospheric central day. If the threshold is exceeded in every level from the stratosphere to the tropospheric reference level at 700 hPa, this event is classified as stratospheric extreme event (weak or strong event) with significant tropospheric response (hereafter Trop events). If the threshold is not exceeded in any of the levels between the stratospheric reference level (30 hPa) and the tropospheric reference level (700 hPa), this stratospheric extreme event is classified to show no significant tropospheric response (hereafter NotTrop events).

With that method, it is ensured that the significant downward propagation of the stratospheric perturbation is given in case of the Trop events. The significant perturbation at each level down to the troposphere following the stratospheric central day strongly suggests that the tropospheric GpH anomaly is related to the stratospheric perturbation (for the Trop events). The date of the maximum (minimum) of the GpH anomaly at 700 hPa during the exceedance of the threshold value is defined as the tropospheric central day. For the NotTrop events, the date of the maximum (minimum) of the GpH anomaly at 700 hPa is used irrespective of whether it exceeds the threshold; in case the anomaly is of different sign to the stratospheric anomaly at 700 hPa, the date of the maximum (minimum) of the GpH anomaly at the lowest level that still shows an anomaly with same sign as the stratospheric signal is used. The propagation duration of stratospheric extreme events of type Trop is calculated via the time difference between the tropospheric central day and the stratospheric central day. The "persistence" of an event is defined here as duration of the longest continuous threshold exceedance in the period 90 days prior and after the tropospheric central day.

This method is applied to each individual simulation, i.e., the REF-B1, the SCN-B2c, and SCN-B2d from E39CA, the three transient REF-B1 simulations from WACCM3.5 and the ERA40 data. It results in four groups of events

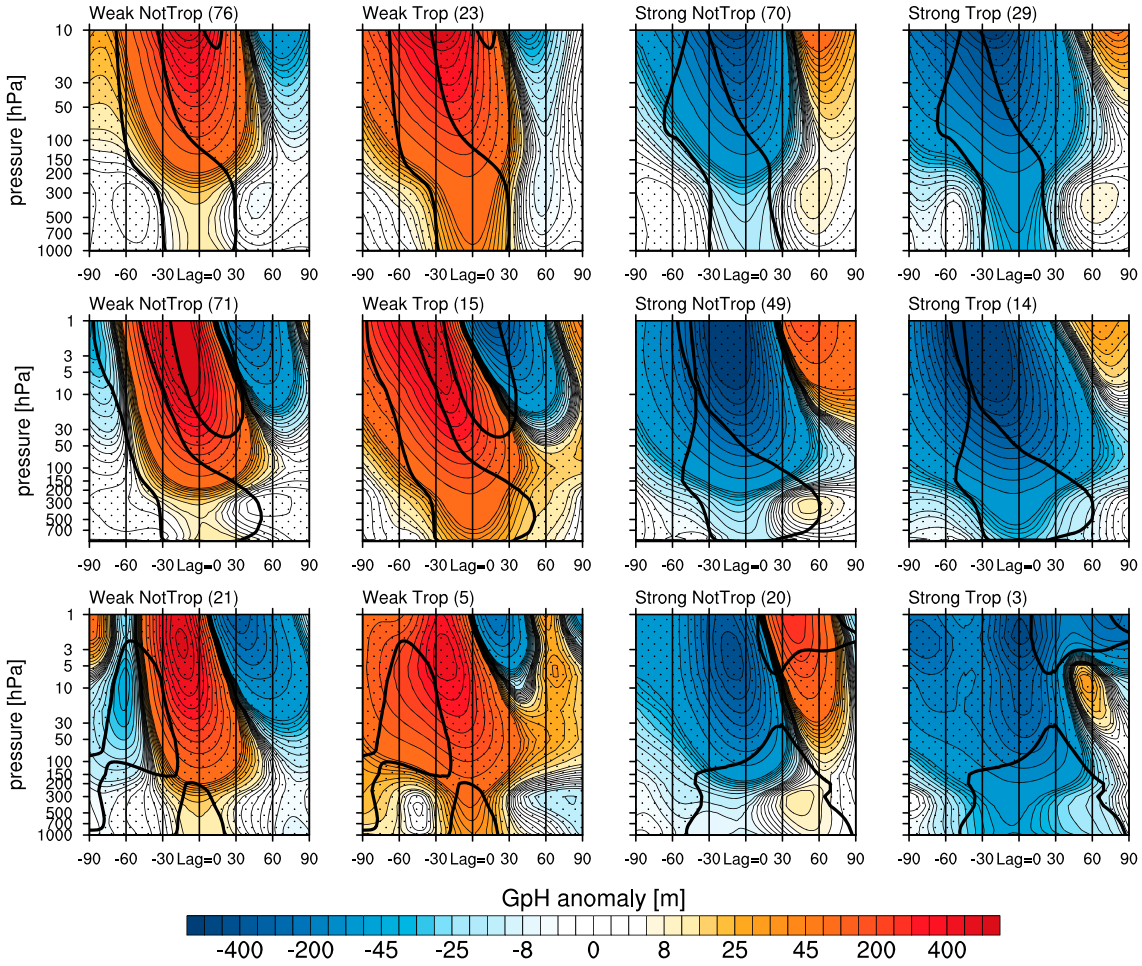

Figure 1. Time development of the GpH anomaly for (top) E39CA events, (center) WACCM3.5 events, and (bottom) ERA40 events. In nonstippled regions, differences between Trop and NTrop are significant on a 99% level with Student's *t* test. Numbers in brackets give number of events that show significant threshold exceedance at 30 hPa pressure level.

(strong and weak vortex events with Trop and NotTrop response each) for each simulation. Based on the tropospheric central day, composites are built for each class of events from all E39CA simulations, all WACCM3.5 simulations and the ERA40 data.

3. Results

The detected stratospheric events occur regularly during northern winter months between mid-December until the end of March for all data sets. No significant differences in the occurrence date between strong and weak vortex events with Trop or NotTrop response can be detected (not shown). Figure 1 shows the time development of the 90 day low-pass-filtered GpH anomaly for the composites of the four groups of events derived from the analysis method described above. The reference day (Lag = 0) corresponds to the tropospheric central day. The numbers in brackets at the top of each chart denotes the number of detected events for each composite. The number of events with significant tropospheric response (type Trop) is much smaller than the number of events without tropospheric impact: for E39CA, WACCM3.5, and ERA40 a fraction of 26%, 19%, and 16% of all events are events with significant tropospheric response, respectively. The average duration of the downward propagation of the signal from the stratosphere (i.e., 30 hPa) into the troposphere (700 hPa) is about 3 weeks in all three data sets, in agreement with findings by *Baldwin and Dunkerton* [2001] and *Kidston et al.* [2015]. Generally, the propagation duration for individual events varies from a few days up to weeks.

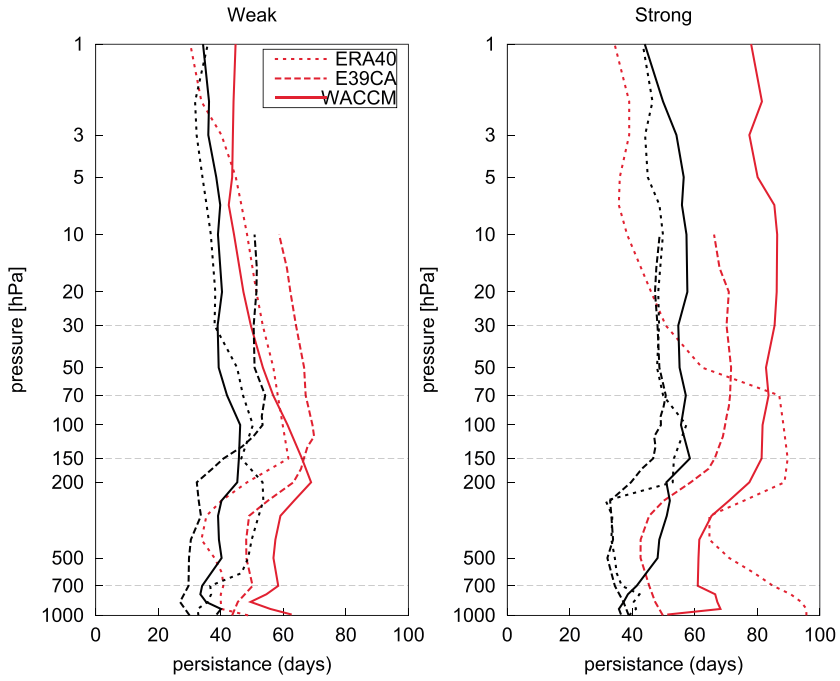

Figure 2. Persistence (i.e., duration of threshold exceedance) of (left) weak and (right) strong events of type Trop (red) and NotTrop (black) for ERA40 (dotted), E39CA (dashed), and WACCM (solid).

For all data sets and both strong and weak events a distinct downward propagation of the GpH anomaly from the stratosphere (beginning at 10 hPa for E39CA and 1 hPa for WACCM and ERA40 data) to the lower troposphere is found for the Trop events. In comparison to that, the signal only reaches the tropopause layer in the NotTrop events. By design of the composites, the signal in the troposphere is statistically different between the Trop and NotTrop events (see black contours in Figure 1). The statistical significant differences between events of type Trop and NotTrop extends around the tropospheric central day for about $\pm$ 30 days, which suggests a certain persistence of the tropospheric anomalies. There also is a statistical significant difference between events of type Trop and NotTrop in the stratosphere already before the tropospheric central day. Both for weak and strong vortex events, the GpH anomaly appears to be more persistent in the stratosphere for Trop events. The persistence is further shown in Figure 2 as a function of height. Generally, the persistence of both weak and strong vortex events agrees relatively well between all three data sets. It can clearly be seen that anomalies persist longer in the stratosphere in the mean of the events with significant tropospheric response (Trop) as compared to those without significant tropospheric response (NotTrop). This is the case both for weak and strong events in all three data sets. The mean persistence at 30, 70, and 150 hPa are also given in Table 1 together with the number of events that contribute to the composites (which decreases with height in the NotTrop case) and the level of significance of the difference between the duration of the Trop and NotTrop events. The difference in the persistence between Trop and NotTrop cases is significant on a level greater than 90% in WACCM and E39CA. In ERA40, the small sample size does not allow for robust statements at some levels (see Table 1).

In WACCM, for weak vortex events, the persistence is found to increase with decreasing height from 30 hPa to about 150 hPa in the Trop cases, while the persistence remains close to constant in the NotTrop cases. The extended persistence in the lower stratosphere can also be seen in Figure 1. In ERA40, a similar behavior is found for weak events, while in E39CA, the maximum persistence is reached already at about 100 hPa. We cannot detect a prolonged persistence in the lower stratosphere for strong events, even though Figure 1 would suggest this for WACCM.

Figure 3 displays the strength (defined as the geopotential height anomaly at the central day) of the stratospheric perturbation in 30 hPa compared to the strength of the tropospheric response in 700 hPa for the four groups of events. The illustrations show that there is a high case-to-case variability of the anomalous stratospheric situations. Events of both types (Trop and NotTrop) span a large range of stratospheric GpH anomalies.

Table 1. Persistence (That Is, Mean Duration of Threshold Exceedance) of Anomalies at 30, 70, and 150 hPa in Days[a]

	Trop	NotTrop	Significance Level
E39CA weak 30 hPa	64(23)	51(76)	0.95
E39CA weak 70 hPa	67(23)	54(63)	0.93
E39CA weak 150 hPa	67(23)	41(56)	0.99
E39CA strong 30 hPa	70(29)	48(70)	0.99
E39CA strong 70 hPa	71(29)	51(60)	0.99
E39CA strong 150 hPa	66(29)	47(53)	0.99
WACCM weak 30 hPa	50(15)	39(71)	0.95
WACCM weak 70 hPa	57(15)	42(52)	0.96
WACCM weak 150 hPa	66(15)	46(36)	0.97
WACCM strong 30 hPa	86(14)	55(49)	0.99
WACCM strong 70 hPa	84(14)	57(43)	0.97
WACCM strong 150 hPa	81(14)	58(33)	0.94
ERA40 weak 30 hPa	53(5)	38(21)	0.97
ERA40 weak 70 hPa	58(5)	47(17)	0.59
ERA40 weak 150 hPa	62(5)	47(15)	0.64
ERA40 strong 30 hPa	51(3)	49(20)	0.16
ERA40 strong 70 hPa	87(3)	50(18)	0.94
ERA40 strong 150 hPa	90(3)	53(14)	0.93

[a]Number in brackets gives number of events that show significant threshold exceedance at the respective level. The fourth column displays the significance level of the difference between Trop and NotTrop.

The correlation coefficient between the GpH anomaly at 30 hPa at the stratospheric central day and the GpH anomaly at 700 hPa at the tropospheric central day for strong and weak polar vortex events of any type is below 0.32 for all three data sets (see Figure 3). This weak correlation between the strength of the perturbation in the stratosphere to the extent of the tropospheric response suggests that the magnitude of signal propagation is independent from the strength of the stratospheric extreme event.

As mentioned in section 2, we used a threshold of 1.5 standard deviations of the GpH anomaly to identify both weak and strong vortex events. It can be seen from Figure 3 that the behavior of stratospheric to

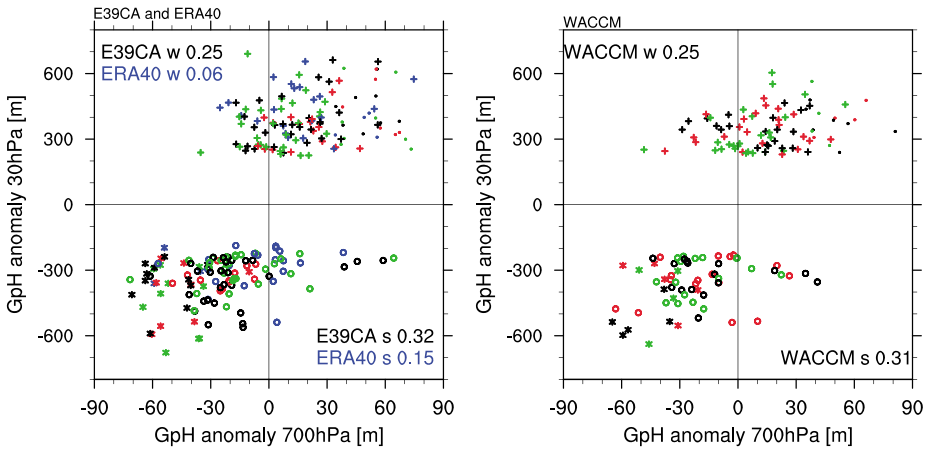

Figure 3. GpH anomaly at 30 hPa plotted against the GpH anomaly at 700 hPa for (left) E39CA and ERA40 and (right) WACCM3.5. Dot (asterisk) denotes weak (strong) events of type Trop and plus (circle) denotes weak (strong) events of type NotTrop. In Figure 3 (left) ERA40 (blue) and E39CA simulations REF-B1 (red) and SCN-B2c (green) and SCN-B2d (black). In Figure 3 (right) WACCM3.5 REF-B1 simulations, with each realization marked in one color. The numbers give the correlation coefficient between the GpH anomaly at 30 hPa and 700 hPa across all weak (w) or strong (s) events.

tropospheric anomalies does not differ when only taking weak GpH anomalies of $+3\sigma$ into account (as was done in *Baldwin and Dunkerton* [2001]): While the sign of tropospheric anomalies becomes more robust for higher stratospheric anomalies (i.e., most events with a tropospheric response of opposite sign occur with weak stratospheric anomalies), the correlation between stratospheric and tropospheric anomalies remains weak when considering only events with GpH anomalies exceeding $+3\sigma$. Thus, our conclusions are not affected by the choice of the lower threshold.

4. Conclusions

This paper presents a new method for the classification of stratospheric extreme events according to the significance of the tropospheric response. This classification is applied to data from two different chemistry-climate models (WACCM and E39CA) and to the ERA40 reanalysis. The model data have the advantage of providing longer data sets which are necessary to allow for robust statements given the strong case-to-case variability between stratospheric extreme events, and the strong tropospheric internal variability. The 45 years of data from ERA40 are already on the short side for the kind of classification we suggest here.

Based on the analyses of polar cap averaged GpH anomalies, it is demonstrated that strong stratospheric signals do not necessarily propagate downward into the middle and lower troposphere. The events with a significant decent of the stratospheric signal down into the troposphere are found to occur less frequently (in about one out of five cases) than those which are only weakly affecting the tropospheric circulation (both for weak or strong vortex events). However, also in the composite mean of the nonpropagating events, the signal in the troposphere is of same sign than the one in the stratosphere; i.e., while we cannot detect a clear significant downward propagation for those events, they might still show a response. This explains why despite the low number of events with significant downward propagation, the composite of all events (as commonly shown) shows a clear signal in the troposphere.

The classification introduced here for both weak and strong events aims to distinguish events according to the significance of the tropospheric anomalies. If it was only due to the tropospheric internal variability whether the tropospheric response to stratospheric extreme events is detectable or not, as suggested by *Gerber et al.* [2009], a classification according to the tropospheric response would be meaningless — and one would expect to find no significant differences of stratospheric events with or without significant tropospheric response. However, as we show here, there are significant differences in the stratospheric anomalies prior to the tropospheric response. In particular, we find that stratospheric extreme events that do show significant downward influence are more persistent throughout the stratosphere. In particular, in the lower stratosphere the persistence is enhanced for the Trop cases. This result is in agreement with *Hitchcock et al.* [2013] and *Gerber et al.* [2009], which both showed a strong relation of the persistence of stratospheric warmings, in particular in the lower stratosphere and the depth of their propagation. In our study we show that this behavior is found not only for stratospheric warmings but also for episodes with an anomalous strong polar vortex.

We showed that the strength of the stratospheric perturbation is only weakly correlated with the strength of the response in the troposphere, i.e., the strength of the stratospheric perturbation does not control how strong the tropospheric response will be or whether a significant response is detected at all. The tropospheric response is influenced by the strong internal variability, which is superimposed on the response, and this likely contributes to the weak correlation. The lack of a correlation between the strength of stratospheric and tropospheric anomalies could also suggest that the state of the troposphere plays an active role in determining whether the stratospheric signal propagates down to the surface, as supported by similar statements in *Thompson et al.* [2006] and *Kunz and Greatbatch* [2013]. Furthermore, we only regard the zonal mean response here, despite the strong zonal asymmetry in the surface response to sudden warmings [*Hitchcock and Simpson*, 2014]. However, as the polar cap GpH very closely resembles the time series of the NAM index (see section 2 and *Baldwin and Thompson* [2009]), the zonal mean GpH represents variability linked to the NAM. It remains to be clarified whether the more localized response might correlate better with the strength of the stratospheric perturbation.

It remains an open question to which degree the large case-to-case variability in the tropospheric response is determined by (a) the properties of the stratospheric perturbation (e.g., its persistence, as evidence presented here suggests) (b) the superimposition of tropospheric internal variability (that might "randomly" mask the response), and (c) the state of the troposphere before or during the stratospheric anomaly (in a more deterministic sense).

Acknowledgments
This work has been supported by the Deutsche Forschungsgemeinschaft (DFG) within the Research Unit SHARP (DA 233/4-1 and DA 233/4-2), by the Federal Ministry of Education and Research (BMBF) within the project "decadal prediction system MiKlip" (01LP1168B), and by the EU-project StratoClim (603557-FP7-ENU.2013.6.1-2). H.G. was funded by the Helmholtz Association under grant VH-NG-1014 (Helmholtz-Hochschul-Nachwuchsforschergruppe MACClim). Model data used in this study can be accessed from the CCMVal2 archive at British Atmospheric Data Archive (BADC) (http://badc.nerc.ac.uk), and ERA40 data are available from the ECMWF (http://www.ecmwf.int).

References

Baldwin, M. P., and T. J. Dunkerton (1999), Propagation of the Arctic Oscillation from the stratosphere to the troposphere, *J. Geophys. Res.*, *104*, 30,937–30,946.
Baldwin, M. P., and T. J. Dunkerton (2001), Stratospheric harbingers of anomalous weather regimes, *Science*, *32*(294), 581–584.
Baldwin, M. P., and D. W. J. Thompson (2009), A critical comparison of stratosphere-troposphere coupling indices, *Q. J. R. Meteorol. Soc.*, *135*(644), 1661–1672, doi:10.1002/qj.479.
Baldwin, M. P., D. W. J. Thompson, E. F. Shuckburgh, W. A. Norton, and N. P. Gillett (2003), Weather from the stratosphere?, *Science*, *301*(5631), 317–319, doi:10.1126/science.1085688.
Dameris, M., et al. (2005), Long-term changes and variability in a transient simulation with a chemistry-climate model employing realistic forcing, *Atmos. Chem. Phys.*, *5*(8), 2121–2145.
Domeisen, D. I. V., L. Sun, and G. Chen (2013), The role of synoptic eddies in the tropospheric response to stratospheric variability, *Geophys. Res. Lett.*, *40*, 4933–4937, doi:10.1002/grl.50943.
Eyring, V., M. P. Chipperfield, M. A. Giorgetta, D. E. Kinnison, E. Manzini, K. Matthes, P. A. Newman, S. Pawson, T. G. Shepherd, and D. W. Waugh (2008), Overview of the New CCMVal reference and sensitivity simulations in support of upcoming ozone and climate assessments and planned SPARC CCMVal, *SPARC Newslett.*, *30*, 20–26.
Garcia, R. R., D. R. Marsh, D. E. Kinnison, B. A. Boville, and F. Sassi (2007), Simulation of secular trends in the middle atmosphere, 1950–2003, *J. Geophys. Res.*, *112*, D09301, doi:10.1029/2006JD007485.
Garfinkel, C. I., D. W. Waugh, and E. P. Gerber (2013), The effect of tropospheric jet latitude on coupling between the stratospheric polar vortex and the troposphere, *J. Clim.*, *26*, 2077–2095.
Gerber, E. P., C. Orbe, and L. M. Polvani (2009), Stratospheric influence on the tropospheric circulation revealed by idealized ensemble forecasts, *Geophys. Res. Lett.*, *36*, L24801, doi:10.1029/2009GL04091.
Hardiman, S. C., et al. (2011), Improved predictability of the troposphere using stratospheric final warmings, *J. Geophys. Res.*, *116*, D18113, doi:10.1029/2011JD015914.
Hardiman, S. C., N. Butchart, T. J. Hinton, S. M. Osprey, and L. J. Gray (2012), The effect of a well-resolved stratosphere on surface climate: Differences between CMIP5 simulations with high and low top versions of the Met office climate model, *J. Clim.*, *25*, 7083–7099.
Hitchcock, P., and I. R. Simpson (2014), The downward influence of stratospheric sudden warmings, *J. Atmos. Sci.*, *71*, 3856–3876.
Hitchcock, P., T. G. Shepherd, and G. L. Manney (2013), Statistical characterization of arctic polar-night jet oscillation events, *J. Clim.*, *26*, 2096–2116, doi:10.1175/JCLI-D-12-00202.1.
Holton, J. R. (2004), *An Introduction to Dynamic Meteorology, Intl. Geophys. Ser.*, 4th ed., Academic Press and Elsevier, San Diego, Calif., and New York.
Kidston, J., A. A. Scaife, S. C. Hardiman, D. M. Mitchell, N. Butchart, M. P. Baldwin, and L. J. Gray (2015), Stratospheric influence on tropospheric jet streams, storm tracks and surface weather, *Nat. Geosci.*, *8*, 433–440, doi:10.1038/NGEO2424.
Kolstad, E. W., T. Breiteig, and A. A. Scaiffe (2010), The association between stratospheric weak polar vortex events and cold air outbreaks in the Northern Hemisphere, *Q. J. R. Meteorol. Soc.*, *136*, 886–893.
Kunz, T., and R. J. Greatbatch (2013), On the Northern Annular Mode surface signal associated with stratospheric variability, *J. Atmos. Sci.*, *70*, 2103–2118.
Limpasuvan, V., D. W. J. Thompson, and D. L. Hartmann (2004), The life cycle of the northern hemisphere sudden stratospheric warmings, *J. Clim.*, *17*, 2584–2596.
Limpasuvan, V., D. L. Hartmann, D. W. J. Thompson, K. Jeev, and Y. L. Yung (2005), Stratosphere-troposphere evolution during polar vortex intensification, *J. Geophys. Res.*, *110*, D24101, doi:10.1029/2005JD006302.
Mitchell, D. M., L. J. Gray, J. Anstey, M. P. Baldwin, and A. J. Charlton-Perez (2013), The influence of stratospheric vortex displacement and splits on surface climate, *J. Clim.*, *26*, 2668–2682.
Nakagawa, K. I., and K. Yamazaki (2006), What kind of stratospheric sudden warming propagates to the troposphere?, *Geophys. Res. Lett.*, *33*, L04801, doi:10.1029/2005GL024784.
Nakicenovic, N., and R. Swart (Eds.) (2000), *Emission Scenarios*, 570 pp., Cambridge Univ. Press, Cambridge, U. K.
Richter, J. H., F. Sassi, and R. R. Garcia (2010), Toward a physically based gravity wave source parameterization in a general circulation model, *J. Atmos. Sci.*, *67*, 136–156, doi:10.1175/2009JAS3112.1.
Rind, D., J. Perlwitz, and P. Lonergan (2005), AO/NAO response to climate change: 1. Respective influences of stratospheric and tropospheric climate changes, *J. Geophys. Res.*, *110*, D12107, doi:10.1029/2004JD005103.
Runde, T. (2012), Ursachen und Wirkung der dynamischen Kopplung von Stratosphäre und Troposphäre, PhD thesis (in German), 147 pp., Ludwig-Maximilian-Universität München, München, Germany.
Scaife, A. A., J. R. Knight, G. K. Vallis, and C. K. Folland (2005), A stratospheric influence on the winter NAO and North Atlantic surface climate, *Geophys. Res. Lett.*, *32*, L18715, doi:10.1029/2005GL023226.
Sigmond, M., J. F. Scinocca, V. V. Kharin, and T. G. Shepherd (2013), Enhanced seasonal forecast skill following stratospheric sudden warmings, *Nat. Geosci.*, *6*, 98–102, doi:10.1038/ngeo1698.
Song, Y., and W. A. Robinson (2006), Dynamical mechanisms for stratospheric influences on the troposphere, *J. Atmos. Sci.*, *61*(14), 1711–1725.
Stenke, A., M. Dameris, V. Grewe, and H. Garny (2009), Implications of Lagrangian transport for simulations with a coupled chemistry-climate model, *Atmos. Chem. Phys.*, *9*, 5489–5504, doi:10.5194/acp-9-5489-2009.
Thompson, D. W. J., M. P. Baldwin, and S. Solomon (2005), Stratosphere-troposphere coupling in the Southern Hemisphere, *J. Atmos. Sci.*, *62*(3), 708–715, doi:10.1175/JAS-3321.1.
Thompson, D. W. J., J. C. Furtado, and T. G. Shepherd (2006), On the tropospheric response to anomalous stratospheric wave drag and radiative heating, *J. Atmos. Sci.*, *63*, 2616–2629.
Uppala, S. M., et al. (2005), The ERA-40 re-analysis, *Q. J. R. Meteorol. Soc.*, *131*(612), 2961–3012, doi:10.1256/qj.04.176.